Pergamon

*Deep-Sea Research I*, Vol. 41, No. 3, pp. 511–530, 1994

0967–0637/94 $7.00 + 0.00

# Lunar-influenced carbonate flux of the planktic foraminifer *Globigerinoides sacculifer* (Brady) from the central Red Sea

JELLE BIJMA,*† CHRISTOPH HEMLEBEN* and KLAUS WELLNITZ*

(*Received* 11 *May* 1993; *in revised form* 24 *June* 1993; *accepted* 24 *June* 1993)

**Abstract**—Two phenomena control the rate of sedimentation of planktic foraminifers: (1) changes in the population structure with time; and (2) size-dependent settling velocities of empty shells. As a result, the total flux and the flux per-size-fraction change significantly during a reproductive cycle. This implies that timing and duration of collection of trap devices are important parameters for interpreting sediment trap-collected samples. Using data on the distribution and abundance of living *Globigerinoides sacculifer* (Brady) from the central Red Sea, a shell flux was modelled. The simulations demonstrate that the sedimentation pattern oscillates on a lunar basis. The foremost result of this study is that the timing of trap deployment within the lunar cycle does not influence the collection if the deployment time of the trap is equal to or a multiple of the reproductive cycle. The effect of two variables on the daily calcite flux was investigated: (1) the reproduction rate; and (2) the length of the reproductive period. A decrease in the reproduction rate shifts the calcite flux maximum from full moon to new moon. A short reproduction period intensifies the full moon flux maximum, especially at high reproduction rates. The total monthly calcite flux, however, is independent of these variables. An estimate for the carbonate flux in the Red Sea due to *G. sacculifer* alone is 1 g $m^{-2}$ $year^{-1}$.

## 1. INTRODUCTION

THE biocoenosis of planktic foraminifers are good indicators of different ocean water masses (BOLTOVSKOY, 1962; CIFELLI, 1962; PARKER, 1960; BÉ, 1977). Under the assumption that their ecological requirements have not changed drastically during the Quaternary (KIPP, 1976), their shells may be used to qualitatively and quantitatively study the paleoclimatic record that is preserved in deep-sea sediments (VINCENT and BERGER, 1981, and refs therein). However, the processes that relate the living assemblage to the sediment are not yet fully understood, although many studies have added substantial knowledge to the understanding of regional, annual and seasonal variability in particle fluxes (e.g. HONJO, 1978; DEUSER and ROSS, 1981; THUNELL and HONJO, 1981; CURRY *et al.*, 1983; THUNELL *et al.*, 1983; REYNOLDS and THUNELL, 1985; DEUSER, 1986; REYNOLDS SAUTTER and THUNELL, 1991). Inter-annual variability can be large, but the high coherence among all constituent particle fluxes indicates that the composition of the settling material is remarkably uniform (DEUSER, 1986). Intra-annual variability in the particle flux originates

*Institut und Museum für Geologie und Paläontologie, Universität Tübingen, Sigwartstraße 10, D-72076 Tübingen, Germany.

†Present address: Alfred Wegener Institut für Polar- und Meeresforschung, Columbusstrasse, D-27568 Bremerhaven, Germany.

from seasonality in foraminiferal productivity (REYNOLDS SAUTTER and THUNELL, 1991). Shorter term variability is more difficult to explain. For example, the monthly recurring reproductive cycle of spinose planktonic foraminifers is thought to add a lunar sequence on top of the seasonal imprint. As our knowledge on the population dynamics of planktic foraminifers is expanding, the effect of short term events on the particle flux can be studied in more detail.

Recently, international efforts (e.g. BOFS, JGOFS) have been undertaken to study the carbon and carbonate flux to the ocean floor. Planktic foraminifers are among the major calcium carbonate producers of the present day and ancient open oceans, and their calcite production may have a significant impact on the global geochemical system. After death or reproduction, the tests sink to the ocean floor. By the time a foraminifer reaches maturity and undergoes gametogenesis, a substantial amount of calcium carbonate has been fixed. The high reproductive potential and the world-wide distribution of planktic species have thus yielded thick sequences of deep-sea sediments.

The reproductive cycle of *G. sacculifer* was shown to be closely related to distinct phases of the moon. Several studies have documented this aspect of the life cycle (ALMOGI-LABIN, 1984; HEMLEBEN *et al.*, 1989; BIJMA *et al.*, 1990; EREZ *et al.*, 1991). In addition, BIJMA and HEMLEBEN (1993) have documented the ontogenetic migration of this species. The zone where growth and development take place is defined as the productive zone. The change in the population structure within the productive zone during one reproductive cycle allows the calculation of a mortality curve. These data are the cornerstone to investigate the variability of the calcite flux of *G. sacculifer* in the central Red Sea on a lunar basis. The second aspect, needed to calculate the calcite flux, is the individual sinking speed.

Several studies were devoted to the settling velocities of particles because sinking speed is important for estimating the residence time of mineralized particles in conjunction with biogeochemical cycles, and for deterministic models that compare the production in the upper water layers with the thanatocoenosis below (BERGER and PIPER, 1972; FOK-PUN and KOMAR, 1983; TAKAHASHI and BÉ, 1984). Previous studies have demonstrated the crucial role of the particle density on the settling velocity of planktic foraminifera. This parameter could only be estimated incompletely. In the present investigation new method was applied to compute the particle density as a function of size.

## 2. MATERIAL AND METHODS

A computer model was developed to simulate the flux of planktic foraminiferal shells on the basis of abundance, mortality and settling velocities. The data of BIJMA and HEMLEBEN (1993) on abundance and mortality of *G. sacculifer* from the central Red Sea were applied and the settling velocities are calculated on the basis of the empirical equation of GIBBS *et al.* (1971).

### 2.1. *Abundance and mortality*

Strictly speaking, BIJMA and HEMLEBEN (1993) constructed a static life table (KREBS, 1978) for each sampling station. However, if we assume that all groups of interbreeding organisms behave similarly, i.e. that the population structure at a certain time is similar at each station, a so called cohort life table may be constructed, which describes the population structure and summarizes the mortality (Table 1).

*Table* 1. *Distribution of size classes* (μm) *in the upper* 80 m *of the water column as a function of the lunar day* (29 = *full moon*) (*in absolute numbers of individuals*)

| Lunar day | Size class | | | | | | | | | | |
|---|---|---|---|---|---|---|---|---|---|---|---|
| | <100 | 100–200 | 200–300 | 300–400 | 400–500 | 500–600 | 600–700 | 700–800 | 800–900 | 900–1000 | Total |
| 3 | 6 | 187 | 69 | 60 | 25 | 22 | 9 | 4 | 1 | 0 | 383 |
| 4 | 137 | 154 | 50 | 29 | 12 | 9 | 6 | 5 | 3 | 0 | 405 |
| 6 | 0 | 13 | 4 | 3 | 2 | 2 | 0 | 1 | 0 | 0 | 25 |
| 7 | 7 | 137 | 42 | 24 | 39 | 29 | 17 | 10 | 9 | 3 | 317 |
| 9 | 13 | 269 | 160 | 80 | 46 | 30 | 22 | 11 | 8 | 2 | 641 |
| 11 | 10 | 111 | 30 | 10 | 11 | 7 | 1 | 0 | 0 | 0 | 180 |
| 13 | 8 | 112 | 46 | 34 | 37 | 44 | 28 | 12 | 2 | 0 | 323 |
| 16 | 0 | 139 | 74 | 56 | 78 | 56 | 42 | 30 | 18 | 5 | 498 |
| 18 | 1 | 16 | 11 | 11 | 12 | 9 | 9 | 3 | 0 | 0 | 72 |
| 19 | 5 | 91 | 15 | 3 | 1 | 1 | 0 | 0 | 0 | 0 | 116 |
| 23 | 0 | 7 | 0 | 2 | 1 | 2 | 0 | 0 | 0 | 0 | 12 |
| 24 | 0 | 3 | 1 | 1 | 1 | 3 | 1 | 0 | 1 | 0 | 11 |
| 25 | 0 | 17 | 1 | 3 | 0 | 0 | 0 | 1 | 1 | 0 | 23 |
| 28 | 25 | 45 | 12 | 5 | 2 | 1 | 2 | 0 | 0 | 0 | 92 |
| 29 | 16 | 72 | 19 | 18 | 16 | 11 | 5 | 0 | 1 | 0 | 158 |
| | 228 | 1373 | 534 | 339 | 283 | 226 | 142 | 77 | 44 | 10 | 3256 |

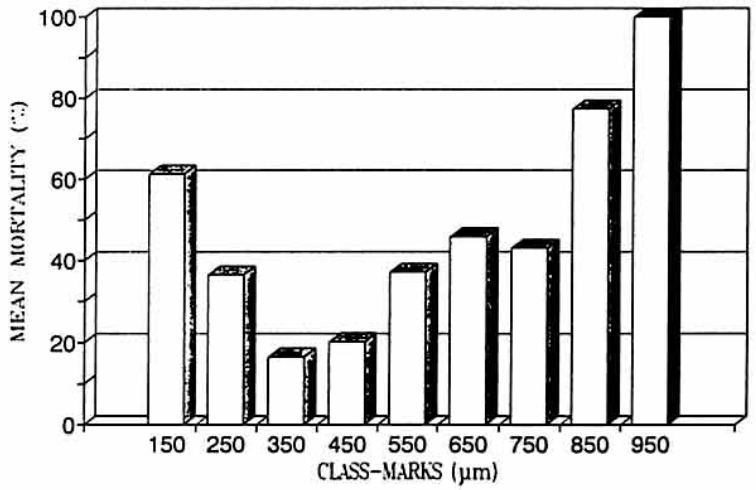


Fig. 1. Mortality bar diagram of *G. sacculifer* from the central Red Sea calculated from the life table and given as percentage of the initial population (>100 μm).

The total number of shells collected in the productive zone (upper 80 m) during one lunar period were added up for each size class. The difference between one size class and the next represents the number of individuals lost through death or gametogenesis. The loss rate was calculated for each size fraction and a mortality curve was constructed (Fig. 1). A mortality curve permits the calculation of the sedimenting shell fraction in successive size classes.

### 2.2. *Settling velocity*

The settling speed of each size class within this fraction was calculated using the empirical relationship of GIBBS *et al.* (1971). It was shown that the formula of GIBBS *et al.* (1971), when used for foraminiferal shells, gave acceptable results (BABA and KOMAR, 1981). Other equations contain parameters that have to be determined experimentally (ROUSE, 1949; KOMAR and REIMERS, 1978; FOK-PUN and KOMAR, 1983) or only allow comparison of two parameters at a time (TAKAHASHI and BÉ, 1984).

### 2.3. *Flux simulation model*

The absolute and relative abundances of nine size fractions were predicted in a hypothetical sediment trap moored at 2500 m depth. The frequency distribution and the daily calcite flux were calculated for different collection times and different starting points within the lunar cycle.

First, the time for each size class to settle to 2500 m depth was calculated in relation to the dynamic viscosity of the water and in relation to the particle density of the test. The dynamic viscosity of seawater changes with temperature, salinity and depth. In the present simulation, the dynamic viscosity was calculated with the equation of MATTHÄUS (1972) using the oceanographical data of *Meteor* cruise 5/5, station 674 (VERCH *et al.*, 1989).

The density of the test was calculated according to the method of SIGNES *et al.* (1993) and OTT *et al.* (1992). Using a digitizing tablet, the outlines of the chambers of a microphotograph of *G. sacculifer* were digitized to reduce the shape to four descriptive parameters; (1) the ratio of radius increase, (2) the path of the log-spiral, (3) the ratio between the distance of the chamber center to the coiling axis and the radius; and (4) the trochospirality. These parameters were then used to reassemble the digitized specimen in the binary bit-space of the computer (OTT *et al.*, 1992). The bits outside the structure were designed a "0", whereas the bits inside were designed a "1". The bit-space was scanned and the resulting volume was calculated. The maximum error for the determination of the shell volume is less than 8%. Weights were calculated using the equation of ANDERSON and FABER (1984). The particle density was then calculated as the sum of the masses of solid calcite (neglecting any possible organic matter) and the water-filled spaces divided by the volume of the test. For the particle density computations, a calcite density of 2.7 g $cm^{-3}$ and a water density of 1.189 g $cm^{-3}$ (Red Sea) were assumed.

Second, using the resulting settling time, the lunar day was traced back at which specimens of each size class were contained in the productive zone. From the life table, the abundance of each size fraction at this specific lunar constellation was obtained. If no data were available for that lunar day, the previous day was taken.

Third, the portion of each size fraction that sinks to the ocean floor at a certain lunar period was computed using the mortality curve. A routine in the program permits to vary the proportion of the population that travels to the ocean floor individually (with and without spines), carried by marine snow and contained in fecal pellets. In this paper we simulate individual transport of shells that have lost their spines.

## 3. RESULTS

The relative frequencies for each size class and the daily calcite flux of *G. sacculifer* were calculated for 16 sediment trap simulation experiments. The collection time was 1, 2 or 3

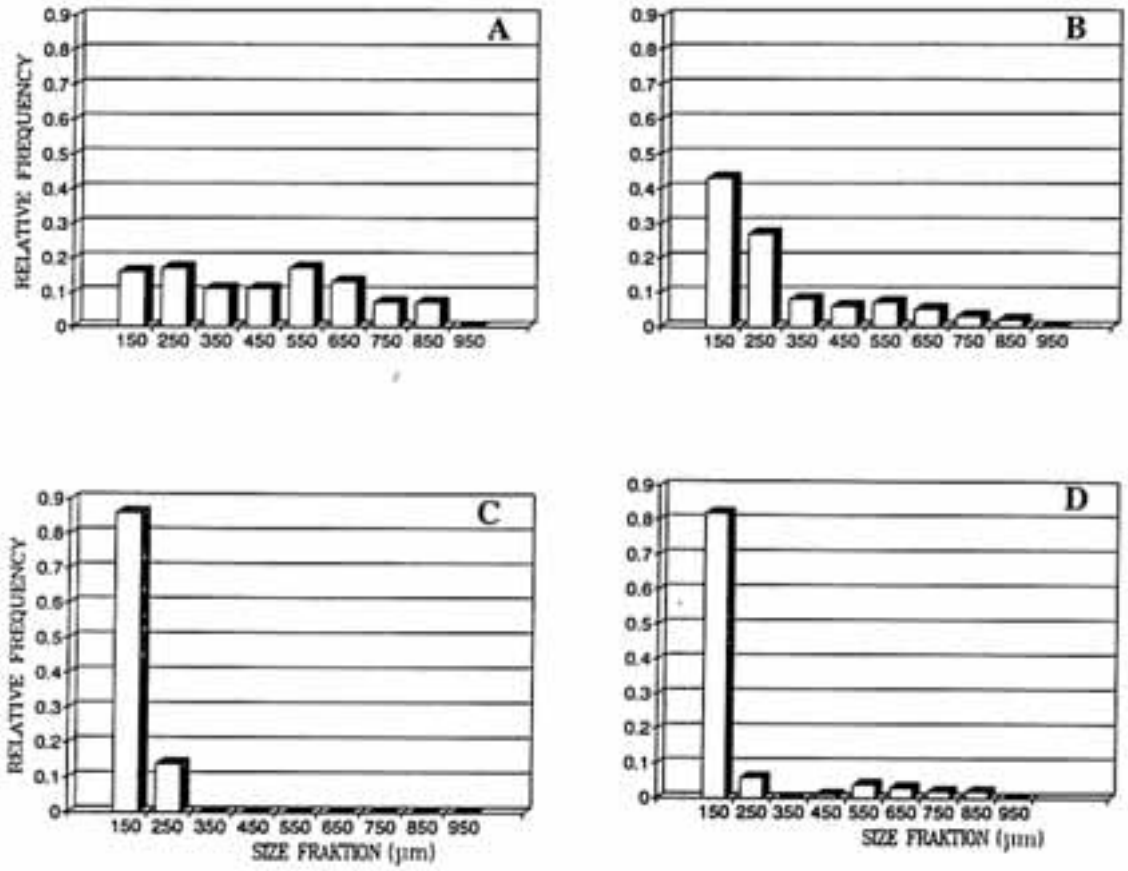


Fig. 2. The relative distribution of *G. sacculifer* in a sediment trap simulation experiment with a collection time of 7 days. (A) Beginning at the 1st lunar day; (B) beginning at the 7th lunar day; (C) beginning at the 14th lunar day; and (D) beginning at the 21st lunar day.

weeks or 29 days, and the trap deployment for each experiment started on the 1st, the 7th, the 14th and the 21st lunar day. The relative foraminiferal shell output is plotted as a function of the size class (Figs 2–5). Three general trends were observed: (1) the relative frequency within each size fraction decreases towards larger sizes; (2) adult specimens are most prominent just after full moon; and (3) if the deployment time increases, the hypothetical yields become more similar. Obviously, when the trap deployment time is shorter than 29 days, the onset of the deployment influences the relative distribution of *G. sacculifer* within each yield, but when the deployment period is 29 days, the timing neither influences the absolute nor the relative yields.

The calcite flux of *G. sacculifer* is not constant but changes drastically in the course of a lunar month. The daily calcite flux (mg calcite $m^{-3}$) was calculated as a function of the lunar cycle using a size–weight relationship for *G. sacculifer* (ANDERSON and FABER, 1984). A total of nine simulations were carried out to understand the effect of the reproduction rate and the length of the reproductive period on the yield. A reproduction rate of 0, 50 or 100% and a reproductive period of 15, 7 and 3 days for each reproduction rate were used. A change in the reproduction rate moves the monthly calcite pulse between new moon and full moon (Figs 6–8). At a low reproduction level, the calcite flux is independent of the reproductive period and shows a maximum around new moon. At a high reproduction level, a calcite flux maximum is found at full moon. At intermediate reproduction rates,

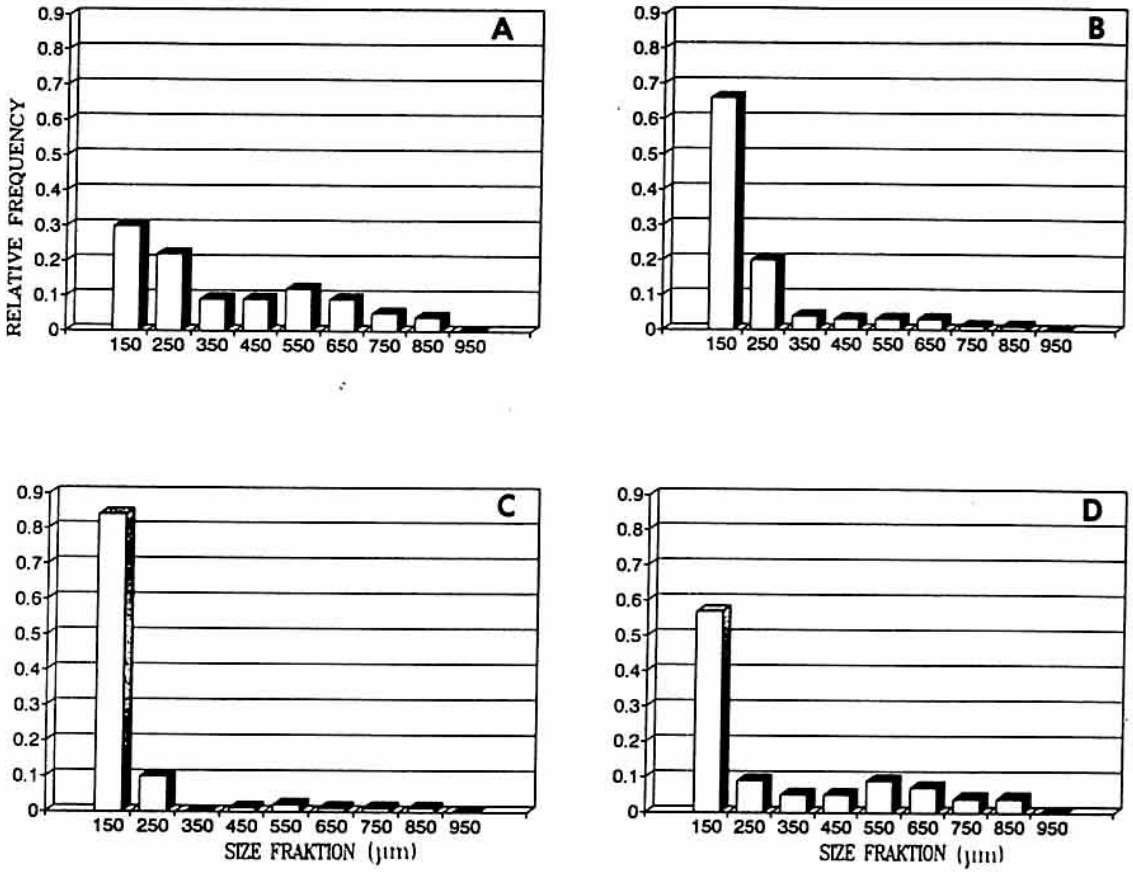


Fig. 3. The relative distribution of *G. sacculifer* in a sediment trap simulation experiment with a collection time of 14 days. (A) Beginning at the 1st lunar day; (B) beginning at the 7th lunar day; (C) beginning at the 14th lunar day; and (D) beginning at the 21st lunar day.

two pulses are present, one around new moon and the other around full moon. Narrowing the reproductive period intensifies the flux maximum at full moon, especially at high reproduction rates.

## 4. DISCUSSION

Our flux simulation program consists of two major routines. The first calculates the settling time of the different size fractions, and the second computes the fraction that settles to the ocean floor.

### 4.1. *Settling time*

The Reynolds numbers for *G. sacculifer* range somewhere between 0.03 and 12.79 (TAKAHASHI, 1984) or 2.3 and 24.4 (FOK-PUN and KOMAR, 1983). Thus, *G. sacculifer* does not follow Stokes' law because Re is too big (0.5 is considered to be an upper limit). Consequently, we employ an empirical equation (GIBBS *et al.*, 1971) to describe the settling of planktic foraminifers. This empirical equation is derived from the sedimentation of glass spheres in water

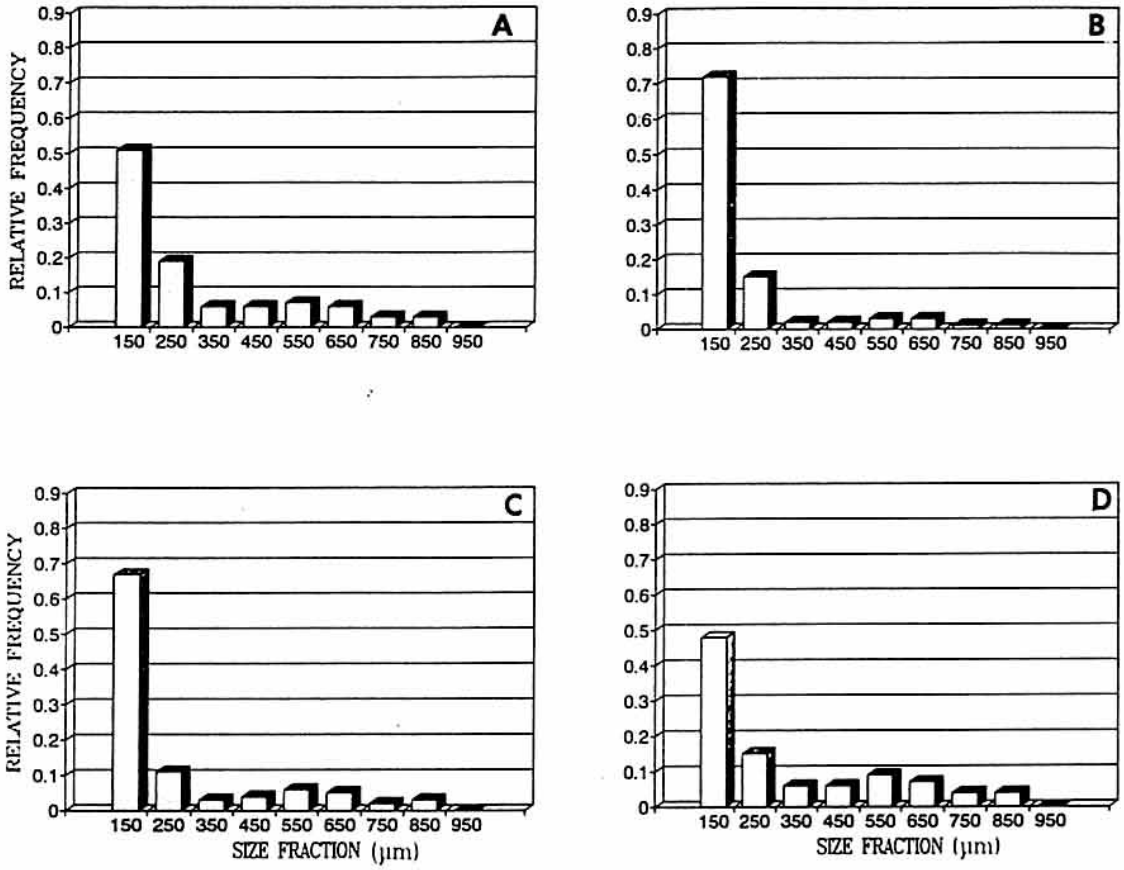


Fig. 4. The relative distribution of *G. sacculifer* in a sediment trap simulation experiment with a collection time of 21 days. (A) Beginning at the 1st lunar day; (B) beginning at the 7th lunar day; (C) beginning at the 14th lunar day; and (D) beginning at the 21st lunar day.

$$SS = \frac{-3\mu + \sqrt{9\mu^2 + gr^2\Theta(\Theta_s - \Theta)(0.015476 + 0.19841r)}}{\Theta(0.011607 + 0.14881r)}$$

where $SS$ = sedimentation speed (cm $s^{-1}$), $\mu$ = dynamic viscosity of water (g $cm^{-1}$, s), $r$ = radius of the sphere (cm), $g$ = gravitation constant (cm $s^{-2}$), $\Theta$ = water density (g $cm^{-3}$), $\Theta_s$ = density of the glass sphere (g $cm^{-3}$).

Two types of parameters are distinguished; independent parameters such as the water density and the gravitation constant and parameters dependent on other factors, such as (1) the dynamic viscosity; (2) the radius; and (3) the density of the shell.

### 4.2. *The dynamic viscosity of seawater*

The effect of pressure on the dynamic viscosity is negligible. We calculated that in the salinity range between 30 and 40%, the change of the dynamic viscosity due to salinity alone is only about 1% and is thus negligible as well. The most important parameter in this respect is water temperature. The dynamic viscosity decreases with increasing temperature. In the Red Sea (Sta. 674) the values range between 0.0087 and 0.0106 (Table 2A). The sedimentation speed decreases with increasing dynamic viscosity. Even within this

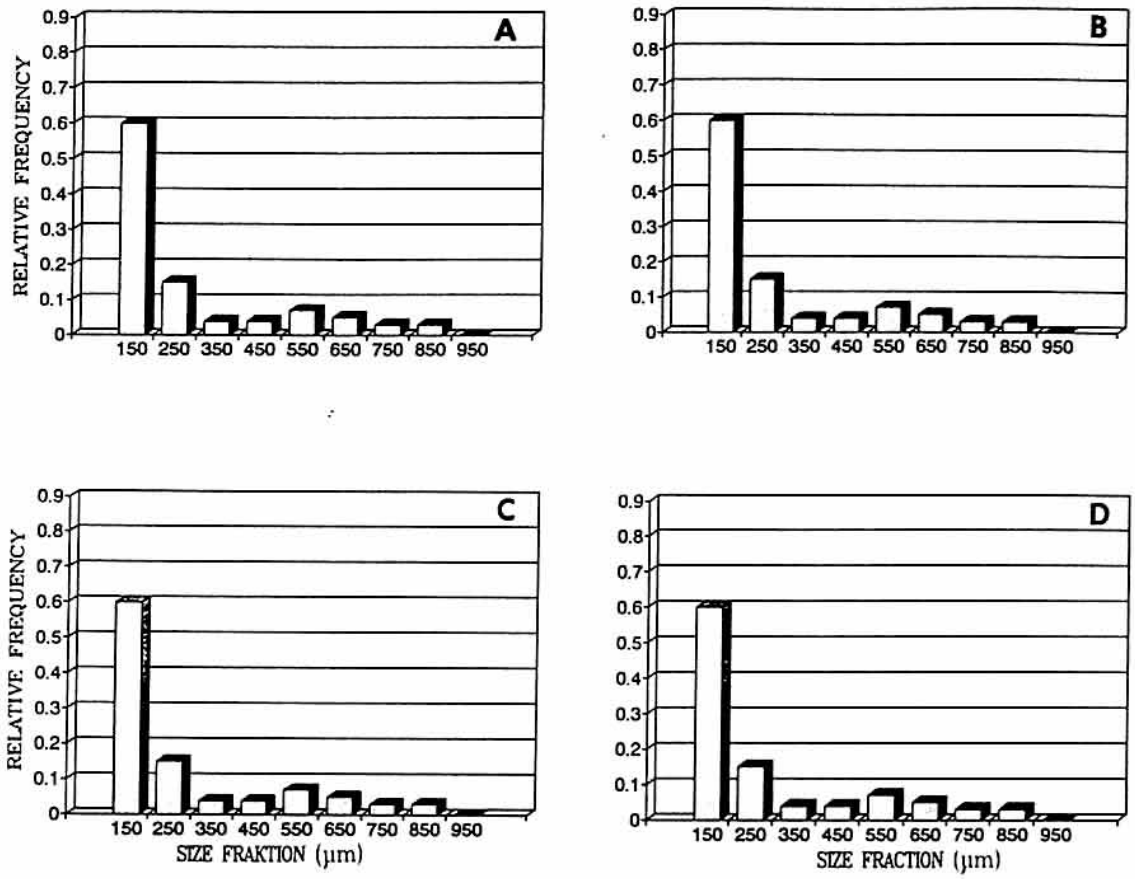


Fig. 5. The relative distribution of *G. sacculifer* in a sediment trap simulation experiment with a collection time of 29 days. (A) Beginning at the 1st lunar day; (B) beginning at the 7th lunar day; (C) beginning at the 14th lunar day; and (D) beginning at the 21st lunar day.

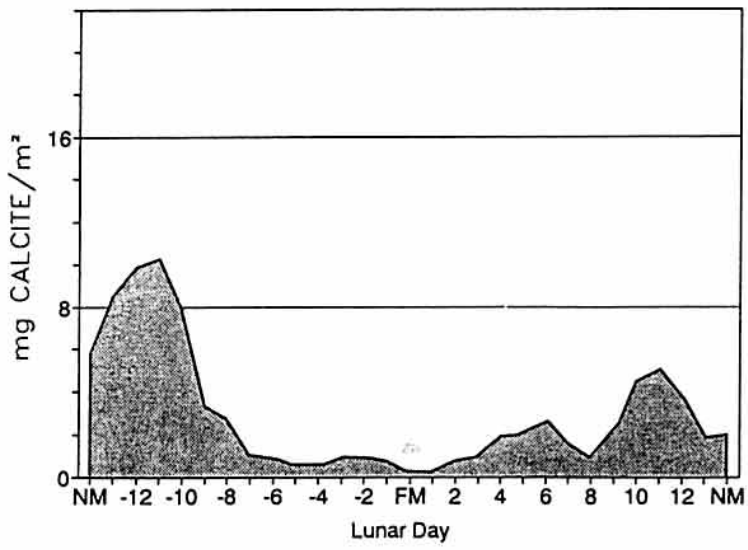


Fig. 6. Hypothetical calcite flux of *G. sacculifer* shells in mg $m^{-2}$ $day^{-1}$ at 2500 m depth in dependence of the lunar cycle at a low reproduction level (0%).

relatively small range, the settling speed of a foraminifer with e.g. a maximum diameter of 400 $\mu$m and a particle density of 1.46 g cm$^{-3}$ changes by about 13%.

The physical parameters in the Red Sea are fairly constant with depth, in contrast to most other seas and oceans. The range of the dynamic viscosities with depth in the Red Sea, therefore, are presumably much smaller (Table 2B; Fig. 9A and B).

### 4.3. *Radius*

The radius depends on the test morphology. In the equation of GIBBS *et al.* (1971) the radius is that of a sphere. For non-spherical foraminifers the nominal radius ($R_n$) may be estimated by axial measurements of the maximum ($D_l$), minimum ($D_s$) and the intermediate diameter ($D_i$):$R_n = 1/2\ (D_l \times D_i \times D_s)^{1/3}$.

Two empirical relationships (in micrometers) are given in the literature. TAKAHASHI and BÉ (1984) calculated for net collected specimens of *G. sacculifer* that $D_n = 10^{0.27} \times D^{0.82}$, where $D = (D_l \times D_i)^{1/2}$. FOK-PUN and KOMAR (1983), on the other hand, calculated for sediment-derived specimens that $D_n = 0.71D_i + 87$, but this relationship loses its validity for small shells because the nominal diameter becomes larger than the largest diameter (Table 3). The morphology of *G. sacculifer* is such that the width of the shell (intermediate diameter) nearly equals the length (maximum diameter) of the preceding growth stage. Using this morphological feature, BIJMA and HEMLEBEN (1993) determined for cultured *G. sacculifer* that $D_l = 1.27D_i + 48$ or $D_i = 0.79D_l - 38$. Substitution of this growth relationship into the equation of TAKAHASHI and BÉ (1984) gives: $R_n = 1/2\ (10^{0.27} \times (D_l(0.79D_l - 38))^{0.41}$.

### 4.4. *Particle density*

A reduction of the particle density of e.g. 0.2 g cm$^{-3}$ causes a 30% slower sedimentation speed (Fig. 10A). Thus, particle density is the most critical parameter for calculating settling speeds. It is, however, also the most controversial one.

Several methods were used to calculate the density of foraminiferal shells. Using Stoke's equation, BERGER and PIPER (1972) estimated the density for foraminiferal shells to be 1.5 g cm$^{-3}$. It should be remembered, however, that foraminifers do not follow Stoke's Law. Using the density of *G. sacculifer* in air (KONTROVITZ *et al.*, 1979) and an estimation of 90% shell porosity (BÉ *et al.*, 1973, 1976), FOK-PUN and KOMAR (1983) calculated a density of 1.72 g cm$^{-3}$ for *G. sacculifer*. This contrasts with the 1.30 g cm$^{-3}$ that was determined experimentally via settling velocities using the equation of ROUSE (1949), drag coefficients and shape factors (SCHULZ *et al.*, 1954; KOMAR and REIMERS, 1978). The value of the drag coefficient in either equation, however, is not exactly computable for non-spherical forms.

The density of the test depends not only on the species but also changes with size. TAKAHASHI and BÉ (1984) used a direct approach, based on shell weight and shell volume. However, they approximated the shell volume by the volume of nominal spheres, using the mean diameter (Fig. 10B). In order to get a better estimate for the volume of a foraminiferal shell, we used a different approach (SIGNES *et al.*, 1993; OTT *et al.*, 1992). In agreement with TAKAHASHI and BÉ (1984) and FOK-PUN and KOMAR (1983), the densities decrease with increasing size (Table 4, Fig. 11). Although the density of the foraminiferal shell decreases with size, the sedimentation speed increases with increasing test size.

TAKAHASHI and BÉ (1984) found a low correlation between the settling velocity and the

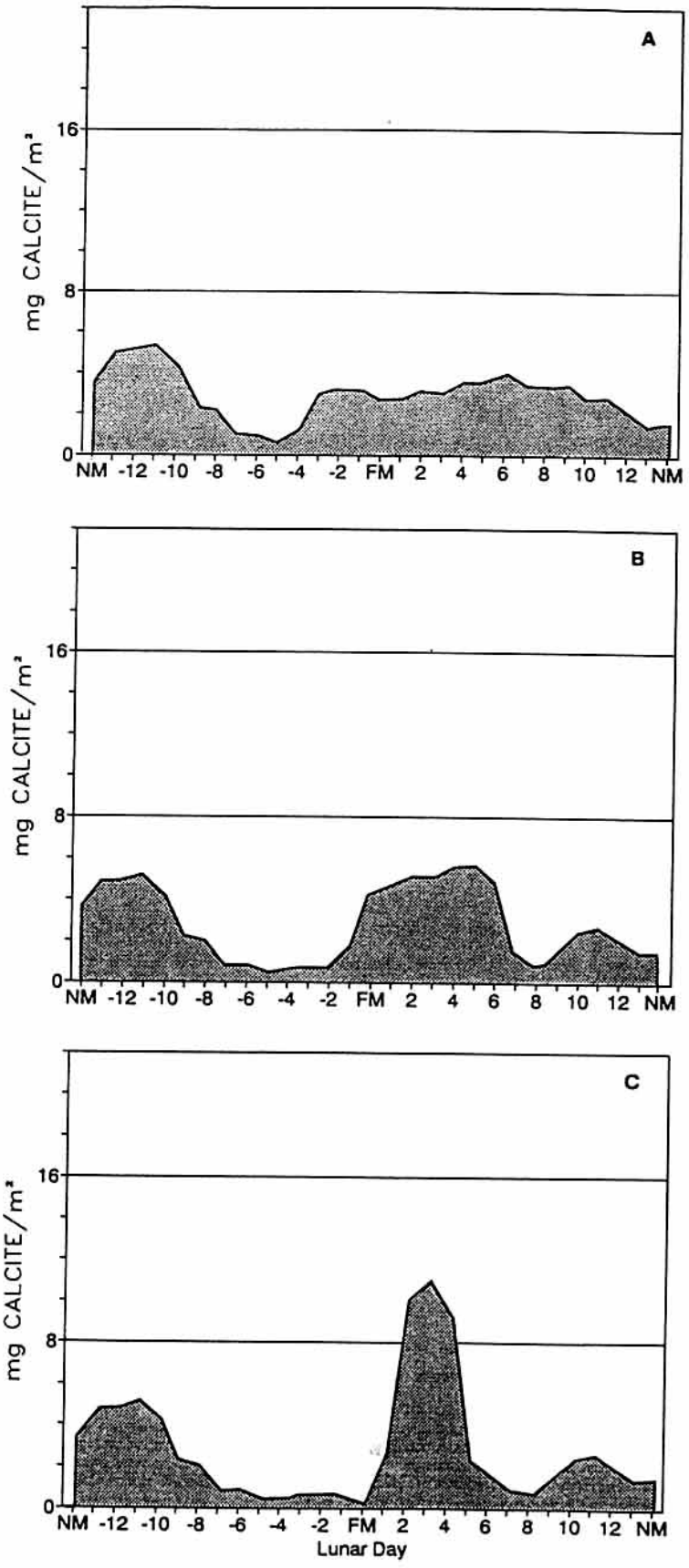
A
B
C
mg CALCITE/m³
16
8
0
NM -12 -10 -8 -6 -4 -2 FM 2 4 6 8 10 12 NM
Lunar Day

density contrast between water and foraminiferal shell, indicating that deriving the density of the shell from the sinking speed is not very accurate. However, although using GIBBS *et al.* (1971) empirical equation to calculate sedimentation speed from particle density data is paradoxical, it is at present the best basis for our model.

### 4.5. *Sedimentation speed*

Our simulated sedimentation speeds may be compared directly to those of TAKAHASHI and BÉ (1984). To compare them with those measured by FOK-PUN and KOMAR (1983), a correction must be applied. The theoretical velocities must be converted to seawater of 3°C, with a density of 1.028 g $cm^{-3}$ and a dynamic viscosity of 0.017 g $cm^{-1}$ s. The conversion factors of DAVIES (1945) for spherical *O. universa*, assuming a shell density of 1.40 g $cm^{-3}$, were used. The equation relating the conversion factor (CF) to size is: $CF = 0.246 \times size^{0.158}$ ($r^2 = 0.99$).

The model compares well with the experimental data of TAKAHASHI and BÉ (1984), and the simulated settling speeds lie in between their "plankton specimens" and ashed specimens from the living assemblage (Fig. 11). Specimens from the sediment yield higher sinking speeds because they have an additional layer of gametogenic calcite and also may be contaminated with fine grained sediments.

To obtain the real settling velocity (*SV*), the sedimentation speed is corrected by a constant factor as suggested by FOK-PUN and KOMAR (1983): $SV = k \times SS$. $k$ compensates for the shape and the roughness of the shell (spinose versus non-spinose, surface texture etc.). For *G. sacculifer*, they computed a correction factor $k \approx 0.8$. As the gross morphology of this species does not change drastically from the late neanic stage onwards (BRUMMER *et al.*, 1987) and we simulated the sedimentation of late neanic to adult stages, $k$ is kept constant.

Whether the spines on sedimenting shells are shed or remain intact depends on how life was terminated. If the specimen underwent gametogenesis, the spines are resorbed and the test is completely empty. If the specimens died, the organic matter can be digested by bacteria and protozoa (within hours after death), but spines remain (HEMLEBEN *et al.*, 1989). TAKAHASHI and BÉ (1984) observed that sinking speeds of spinose specimens are approximately three-fold slower than those of non-spinose species because spines significantly increase the drag coefficient. A maximum drag coefficient was observed for small *G. sacculifer*. Stratified plankton samples have demonstrated that with increasing depth the percentage of empty shells increases drastically (BIJMA and HEMLEBEN, 1993): Almost all spinose shells that arrive at 3200 m in the Sargasso Sea have shed their spines and are empty (DEUSER *et al.*, 1981). Living individuals of planktic foraminifers comprise up to 66% of the shell population in the upper 200 m in the Pacific and only approximately 10% at greater depth (BISHOP *et al.*, 1980). In the equatorial Atlantic an average of about 20%

Fig. 7. Hypothetical calcite flux of *G. sacculifer* shells in mg $m^{-2}$ $day^{-1}$ at 2500 m depth in dependence of the lunar cycle at an intermediate reproduction level (50%). (A) Reproductive period from 1 week before to 1 week after full moon; (B) reproductive period from 3 days before to 3 days after full moon; and (C) reproductive period from 1 day before to 1 day after full moon.

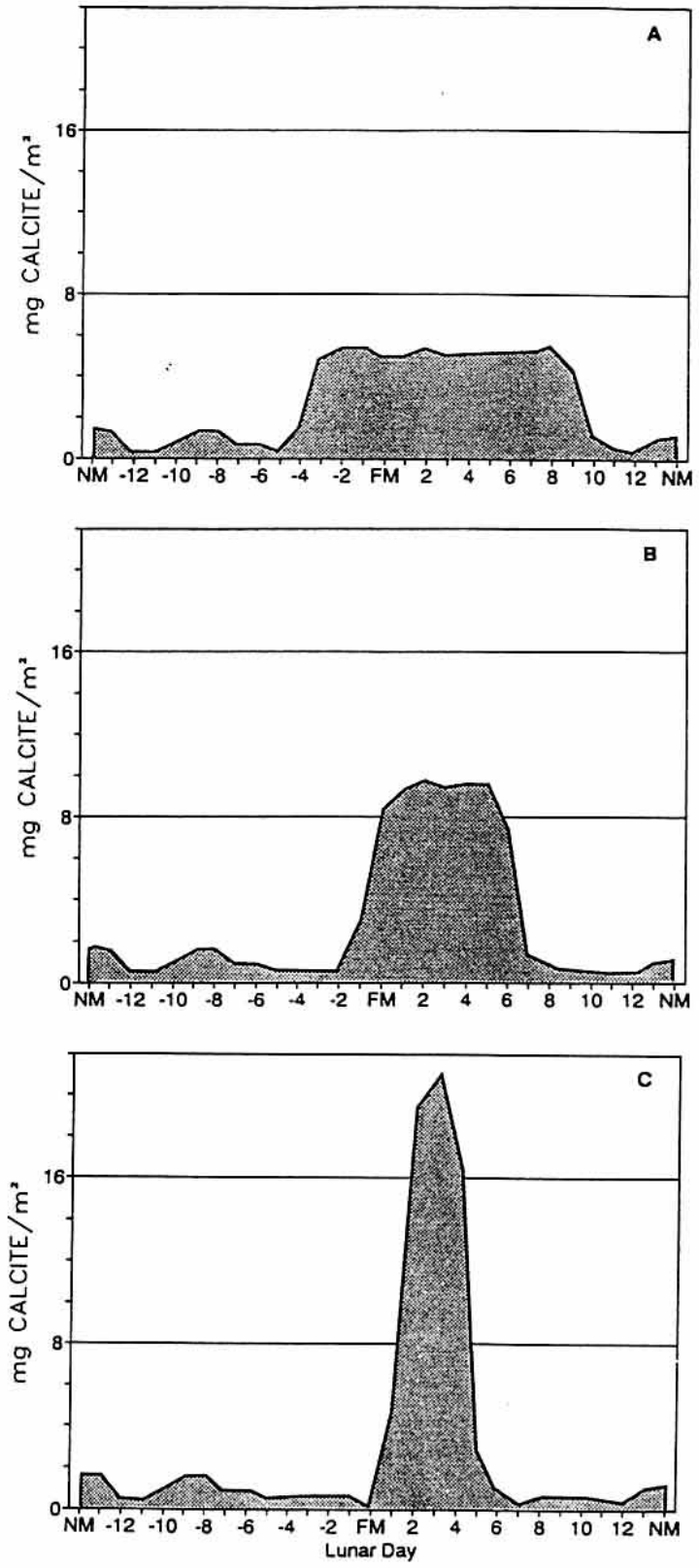


Fig. 8. Hypothetical calcite flux of *G. sacculifer* shells in mg $m^{-2}$ $day^{-1}$ at 2500 m depth in dependence of the lunar cycle at a high reproduction level (99%). (A) Reproductive period from 1 week before to 1 week after full moon; (B) reproductive period from 3 days before to 3 days after full moon; and (C) reproductive period from 1 day before to 1 day after full moon.

*Table 2. The dynamic viscosity of seawater calculated with the equation of* MATTHÄUS (1972). (A) *Data from* VERCH et al. (1989) *for the Red Sea at Sta.* 674. (B) *Data from* DIETRICH et al. (1975) *for the Atlantic* (13°*N*)

| (A) Depth | Temperature | Salinity | Dynamic viscosity |
|---|---|---|---|
| 0 | 30.7 | 38.9 | 0.0087 |
| 100 | 24.0 | 40.0 | 0.0101 |
| 200 | 21.9 | 40.4 | 0.0105 |
| 300 | 21.7 | 40.6 | 0.0106 |
| 400 | 21.7 | 40.6 | 0.0106 |
| 500 | 21.7 | 40.6 | 0.0106 |
| 600 | 21.7 | 40.6 | 0.0106 |
| 700 | 21.7 | 40.6 | 0.0106 |
| 800 | 21.7 | 40.6 | 0.0106 |
| 900 | 21.7 | 40.6 | 0.0106 |
| 1000 | 21.7 | 40.6 | 0.0106 |
| 1100 | 21.7 | 40.6 | 0.0106 |
| 1200 | 21.7 | 40.6 | 0.0106 |
| 1300 | 21.7 | 40.6 | 0.0106 |
| 1400 | 21.7 | 40.6 | 0.0106 |
| 1500 | 21.7 | 40.6 | 0.0106 |
| 1750 | 21.7 | 40.5 | 0.0106 |
| 2000 | 21.8 | 40.5 | 0.0106 |
| 2250 | 21.8 | 40.5 | 0.0106 |
| 2500 | 21.9 | 40.5 | 0.0105 |

| (B) Depth | Temperature | Salinity | Dynamic viscosity |
|---|---|---|---|
| 0 | 25.0 | 36 | 0.0098 |
| 60 | 20.0 | 36 | 0.0109 |
| 120 | 15.0 | 36 | 0.0123 |
| 350 | 10.0 | 35 | 0.0139 |
| 1240 | 5.0 | 35 | 0.0161 |
| 1700 | 4.0 | 35 | 0.0166 |
| 2000 | 3.5 | 35 | 0.0169 |
| 2600 | 3.0 | 35 | 0.0171 |
| 3400 | 2.5 | 35 | 0.0173 |

of the spinose forms had their spines preserved in sediment traps between 3000 and 5582 m depth. In comparison, the preservation in the central Pacific is less, and approximately 10% had their spines preserved in a sediment trap array moored between 3755 and 5068 m depth (THUNELL and HONJO, 1981). Thus about 80–90% of the spinose shells that sink to the ocean floor are empty and have lost their spines.

Transport, attached to detrital phytoplankton aggregates or contained in fecal pellets, may speed up the sinking velocity. Although scarce, most data suggests that transport of individual particles is the major sinking mode of late neanic and adult foraminiferal shells (TAKAHASHI and BÉ, 1984; Hemleben, unpublished data). For this reason, the sinking speeds herein were calculated for specimens that have both shed their spines and sink as single particles.

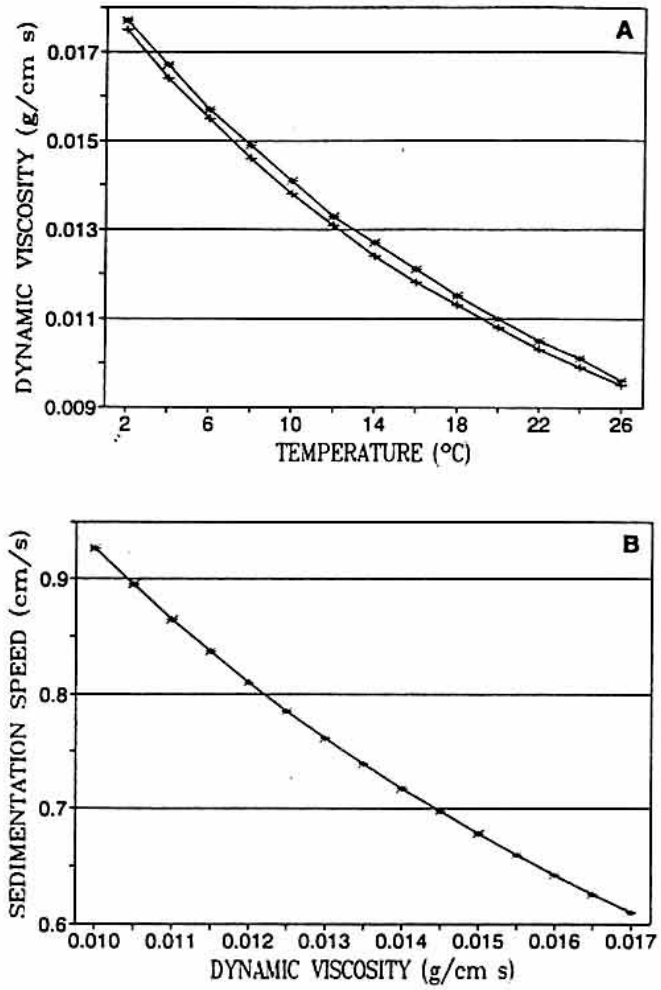


Fig. 9. (A) Dynamic viscosity (in g $cm^{-1}$. s) in dependence of the water temperature at 30‰ (+) and 40‰ (×). (B) Sedimentation speed in dependence of the water viscosity computed after the equation of GIBBS *et al.* (1972) for foraminifers with a maximum diameter of 400 $\mu$m and a density of 1.46 g $cm^{-3}$.

*Table* 3. *Comparison of nominal diameter* ($D_n$) *according to the relationship* $D_n = 10^{0.27} \times (0.79D_l - 37.8) \times D_l)^{0.41}$ *and calculated with two other empirical relationships*, * *based on* TAKAHASHI *and* BÉ (1984), †*based on* FOK-PUN *and* KOMAR (1983). BIJMA *and* HEMLEBEN (1993) *calculated for cultured* G. sacculifer *that* $D_l = -1.273D_i + 48$. *All units are* $\mu$m

| $D_l$ | $D_i$ | $D_n$ | $D_n$* | $D_n$† |
|---|---|---|---|---|
| 175 | 100 | 102 | 102 | 158 |
| 302 | 200 | 170 | 170 | 229 |
| 429 | 300 | 232 | 232 | 300 |
| 556 | 400 | 290 | 290 | 371 |
| 683 | 500 | 346 | 346 | 442 |
| 810 | 600 | 400 | 400 | 513 |

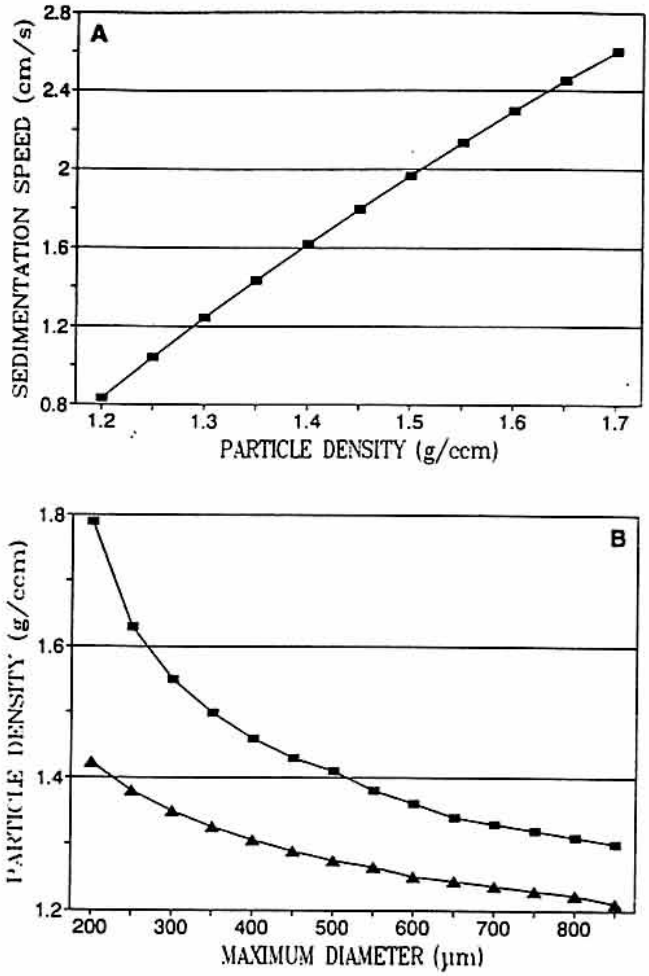


Fig. 10. (A) Sedimentation speed in dependence of the density of the foraminifer computed after the equation of GIBBS *et al.* (1972) for foraminifers with a nominal diameter of 400 $\mu$m and a dynamic viscosity of 0.016 g $cm^{-1}$ $s^{-1}$. (B) Relationship between size and density of *G. sacculifer* calculated on bases of computer models (filled squares). Data of TAKAHASHI and BÉ (1984) are indicated by filled triangles.

## 4.6. *Calculation of daily flux*

The settling time was calculated from the size-dependent sedimentation speed (Table 5) and the depth at which a hypothetical sediment trap was moored (2500 m). Thus, the lunar day can be traced back to that time at which specimens of a certain size class started to sink.

The portion of each size class that is actually transported to the seafloor is calculated from the mortality histogram (Fig. 1). However, this mortality histogram represents the average mortality of each size class during the life cycle, i.e. combined mortality through death or gametogenesis. Under natural conditions only few specimens terminate their lives by undergoing gametogenesis. For immature specimens, empty shell output is due to natural death and predation (BIJMA and HEMLEBEN, 1993). Although the mortality differs for each size class (being higher for smaller fractions), we assume that death rates within each fraction is constant with time, i.e. independent of the lunar cycle. For mature specimens, empty shell output is mainly caused by gametogenesis. Reproduction rates are not constant with time. Gametogenesis mainly occurs around full moon (BIJMA *et al.*, 1990; BIJMA and HEMLEBEN, 1993). In other words, the loss rates obtained from the mortality

*Table 4. The density for* G. sacculifer *calculated on the basis of weight and volume. Shell volumes were estimated using a new method (OTT* et al., 1992). *The density of calcite* = 2.7 g $cm^{-3}$ *and the water density* = 1.189 g $cm^{-3}$. *Shell weights were calculated after ANDERSON and FABER* (1984). *For explanation see text*

| Shell size ($\mu$m) | Shell volume ($\times 10^{-3}$ $mm^3$) | Volume | | Calcite weight ($\mu$g) | Water weight ($\mu$g) | Specific density (g $cm^{-3}$) |
|---|---|---|---|---|---|---|
| | | Calcite ($\times 10^{-3}$ $mm^3$) | Water ($\times 10^{-3}$ $mm^3$) | | | |
| 142 | 0.6 | 0.6 | 0.0 | 1.5 | 0.0 | 2.67 |
| 171 | 1.0 | 0.6 | 0.4 | 1.7 | 0.4 | 2.10 |
| 205 | 1.7 | 0.8 | 0.9 | 2.2 | 0.9 | 1.81 |
| 246 | 3.0 | 1.1 | 1.9 | 3.1 | 1.9 | 1.66 |
| 295 | 5.2 | 1.7 | 3.5 | 4.6 | 3.6 | 1.57 |
| 354 | 9.0 | 2.6 | 6.4 | 7.0 | 6.6 | 1.51 |
| 425 | 5.6 | 4.0 | 11.6 | 10.8 | 11.8 | 1.45 |
| 509 | 26.9 | 6.2 | 20.7 | 16.7 | 21.2 | 1.41 |
| 611 | 47.5 | 9.5 | 38.0 | 25.7 | 38.9 | 1.36 |
| 734 | 80.1 | 14.5 | 65.6 | 39.2 | 67.0 | 1.33 |
| 880 | 138.0 | 22.0 | 116.0 | 59.4 | 119.1 | 1.29 |

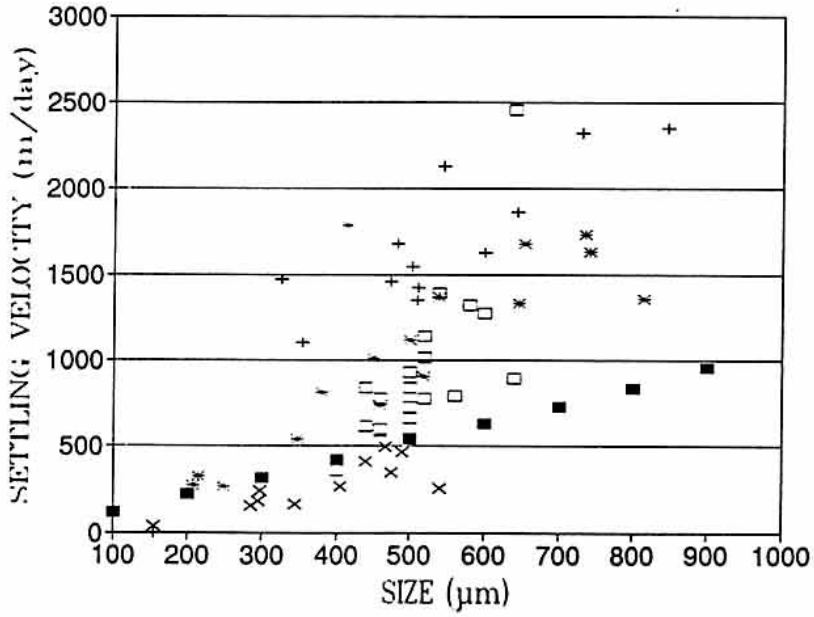


Fig. 11. The settling velocity as a function of maximum test diameter (closed squares). The settling speed of S-specimens (+), P-specimens (x) and A-specimens (*) of TAKAHASHI and BÉ (1984) and corrected settling speeds of FOK-PUN and KOMAR (1983) (open squares) are given for comparison.

curve for mature specimens are the averaged empty shell production through predation, death and gametogenesis. Thus the flux of mature specimens, calculated from the mortality curve (total flux), underestimates the real flux during the reproductive period of *G. sacculifer* and overestimates the real flux in the complementary period. BIJMA and HEMLEBEN (1993) showed that maturation in *G. sacculifer* occurs from 366 $\mu$m onward, which corresponds to a sieve size of 250 $\mu$m.

*Table 5. Calculated sedimentation speed (in* m $day^{-1}$*) and sedimentation time to* 2500 m *(in* days*) for* G. sacculifer. *For explanation see text. Weight is calculated according to the equation of* ANDERSON *and* FABER (1984)

| Size ($\mu$m) | Weight ($\mu$g) | Sedimentation speed (m $day^{-1}$) | Sedimentation time (days) |
|---|---|---|---|
| 100 | 1.51 | 115 | 21.6 |
| 200 | 2.13 | 220 | 11.4 |
| 300 | 4.75 | 312 | 8.0 |
| 400 | 9.37 | 422 | 5.9 |
| 500 | 15.99 | 537 | 4.7 |
| 600 | 24.61 | 627 | 4.0 |
| 700 | 35.23 | 726 | 3.4 |
| 800 | 47.85 | 832 | 3.0 |
| 900 | 62.47 | 955 | 2.6 |

The contribution of reproduction to the shell export must be calculated for each mature size fraction. The relationship between the reproduction rate and size can be approximated by an S-shaped curve (BIJMA and HEMLEBEN, 1993). Multiplication of the mean total flux of a size class with the percentage of gametogenic specimens for this size class gives the flux due to reproduction alone, i.e. the flux overestimation in the non-reproductive period. As a first approximation, we assume that the response to the stimulus that triggers gametogenesis is constant during the reproductive period. Consequently, the absolute number of gametogenic specimens calculated above is added in equal parts to each day within the reproductive period and subtracted in equal parts from the complementary period.

### 4.7. *Predictions of the model*

The frequency distribution in a sediment trap sample depends on the onset of trap deployment within the lunar cycle and on the collecting time (Figs 2–5). The settling time of small specimens is much longer than that of large specimens (Fig. 11). Consequently, specimens in a sample may derive from different reproductive cycles. We assume that consecutive reproductive cycles are similar, i.e. that the production structure in the productive zone is comparable and that the mortality curves are the same.

If the collecting time equals one reproductive cycle, the timing does not influence the frequency distribution (Fig. 5). In sediment traps with a shorter collection time, the frequency distribution of the collected shells does not represent a complete "generation" (Figs 2–4).

As a result of their lunar reproductive rhythm, pulses of calcite are produced (Figs 6–8). The frequency of gametogenesis and the period of reproduction have an important impact on this calcite flux. In the hypothetical situation where no gametogenesis occurs, peaks occur around new moon. Obviously, the length of the reproductive period does not influence the flux in this case (Fig. 6). Although, numbers are high in the beginning, specimens are small. By the end of the cycle, specimens have fixed much more calcite but

their numbers have decreased. Thus a *G. sacculifer* population fixes most calcite in the middle of its reproductive cycle. This is in agreement with THUNELL *et al.* (1983), who found that the 250–500 $\mu$m size fraction contributes between 70 and 80% of the foraminiferal flux.

When 50% of all size fractions >366 $\mu$m undergo gametogenesis, two flux maxima emerge, one around new moon and one around full moon (Fig. 7A–C). If all specimens >366 $\mu$m undergo gametogenesis, only the flux-pulse around full moon remains. In both cases the pulse is stronger if the reproductive period is shorter (Fig. 8A–C). As a first approximation we assume that gametogenesis is restricted to 1 week before and after full moon. Analysis of the flux assemblage showed that most specimens >350 $\mu$m have undergone gametogenesis (BIJMA and HEMLEBEN, 1993), we therefore assume a strong flux-pulse around full moon and a weaker flux around new moon. Unfortunately, no real sediment trap data with short enough collection intervals are available to compare with our simulation data.

The *G. sacculifer* calcite flux in the central Red Sea over a period of 29 days equals 83 mg $m^{-2}$ (Figs 6–8). As we do not correct for dissolution, this number represents approximately the monthly production of *G. sacculifer*. Then the yearly production sums up to 1.045 g $m^{-2}$. If we assume that the density of *G. sacculifer* in the central Red Sea is representative for the Red Sea as a whole and that the productive surface area of the Red Sea is about 424,000 $km^2$, then a yearly calcite flux contributed by *G. sacculifer* adds up to 443,08 ktons $year^{-1}$. If the whole calcite producing plankton community is considered, the total flux is much higher. In the Panama basin, for instance, total planktic foraminifers >125 $\mu$m account for between 28 and 34% of the total carbonate flux (THUNELL *et al.*, 1983). In our Red Sea sediment samples, the size fraction < 125 $\mu$m constitutes 88% by weight. Thus, only 12% of the sample belongs to the size fraction >125 $\mu$m, of which *ca.* 10% can be assigned to *G. sacculifer*. On the other hand the carbonate content in the size fraction >125 $\mu$m measures between 90 and 100% (equal to total planktic foraminiferal fauna). We can thus estimate that the total flux > 125 $\mu$m must be approximately 10.45 g $m^{-2}$ $year^{-1}$. This is in good agreement with other known values (THUNELL *et al.*, 1983). In a recent paper on transport and carbon exchange in the Red Sea METZL *et al.* (1989) estimated a calcium carbonate flux of $600 \times 10^9$ Mol $year^{-1}$ which is 60,000 ktons $year^{-1}$. Using our data we calculate *ca.* 4430.8 ktons $year^{-1}$ for the fraction >125 $\mu$m and 16246.3 ktons of carbonate within the fraction <125 $\mu$m. This adds up to 20677.1 ktons $year^{-1}$ of total carbonate flux in the Red Sea. This is much less than the values given by METZL *et al.* (1989), but more realistic, we believe.

## 5. CONCLUSIONS

(1) The absolute and relative flux per size fraction as well as the daily calcite flux (mg $m^{-2}$) of *Globigerinoides sacculifer* (Brady) changes significantly as a function of the synodic lunar cycle. Consequently, *G. sacculifer* produces pulses of calcite, rather than a steady particle rain.

(2) If the collection intervals of a sediment trap are set equal to, or are a multiple of, the reproductive cycle, the onset of deployment within the lunar cycle will not influence the relative, the absolute, or the total, calcite flux.

(3) The total calcite flux of one reproductive cycle is independent of the reproduction rate and of the length of the reproductive period.

(4) A thorough knowledge of the population dynamics of biogenic carbonate producers is required to accurately estimate the potential carbonate flux.

*Acknowledgements*—Master and crew of the FS "*Meteor*" and the cruise-leaders H. Thiel (Leg two) and H. Weikert (Leg five) are gratefully acknowledged for excellent cooperation. We further want to thank M. Rolke (Leg two) and A Auras (Leg five) for shipboard assistance and D. Mühlen and G. Höckh for sample analysis and measurement. For the generous consent to use the multiple open and closing gear we want to thank H. Weikert and J. Lenz. G. J. Boekschoten, G. J. A. Brummer, J. D. Milliman, K. M. Towe and two anonymous reviewers read and criticized the manuscript. The financial support of the DFG (SPP Meteorauswertung, He 697/7) is gratefully acknowledged.

## REFERENCES

ALMOGI-LABIN A. (1984) Population dynamics of planktic Foraminifera and Pteropoda—Gulf of Aqaba, Red Sea. *Proceedings of the Koninklijke Nederlandse Akademie van Wetenschappen*, Series B, **87(4)**, 481–511.

ANDERSON O. R. and W. W. FABER JR (1984) An estimation of calcium carbonate deposition rate in planktonic foraminifera *Globigerinoides sacculifer* using 45-Ca as a tracer: a recommended procedure for improved accuracy. *Journal of Foraminiferal Research*, **14**(4), 303–308.

BABA J. and P. D. KOMAR (1981) Measurements and analysis of settling velocities of natural sand grains. *Journal of Sedimentary Petrology*, **51**, 631–640.

BÉ A. W. H. (1977) An ecological, zoogeographic and taxonomic review of recent planktonic foraminifera. In: *Oceanic micropaleontology*, Vol. 1, A. T. S. RAMSAY, editor, Academic Press, London, pp. 1–100.

BÉ A. W. H,. S. M. HARRISON, W. E. FRERICHS and M. E. HEIMAN (1976) Variability in test porosity of *Orbulina universa* d'Orbigny at two Indian Ocean localities. In: *Progress in micropaleontology*, Y. TAKAYANAGI and T. SAITO, editors, The American Museum of Natural History, New York, pp. 1–9.

BÉ A. W. H., S. M. HARRISON and L. LOTT (1973) *Orbulina universa* d'Orbigny in the Indian Ocean. *Micropaleontology*, **19**, 150–192.

BERGER W. H. and D. J. W. PIPER (1972) Planktonic Foraminifera: differential settling, dissolution and redeposition. *Limnology and Oceanography*, **17**(2), 275–287.

BIJMA J., J. EREZ and CH. HEMLEBEN (1990) Lunar and semi-lunar reproductive cycles in some spinose planktonic foraminifers. *Journal of Foraminiferal Research* **20**(2), 117–127.

BIJMA J. and CH. HEMLEBEN (1993) Population dynamics of the planktic foraminifer *Globigerinoides sacculifer* (Brady) from the central Red Sea. *Deep-Sea Research I*, **41**, 485–510.

BISHOP J. K. B., R. W. COLLIER, D. R. KETTEN and J. M. EDMOND (1980) The chemistry, biology and vertical flux of particulate matter from the upper 1500 meters of the Panama Basin in the equatorial Pacific Ocean. *Deep-Sea Research*, **27**, 615–640.

BOLTOVSKOY E. (1962) Planktonic foraminifera as indicators of different water masses in the south Atlantic. *Micropaleontology*, **8**(3), 403–408.

BRUMMER G. J. A., CH. HEMLEBEN and M. SPINDLER (1987) Ontogeny of extant spinose planktonic foraminifera (Globigerinidae): A concept exemplified by *Globigerinoides sacculifer* (Brady) and *G. ruber* (d'Orbigny). *Marine Micropaleontology*, **12**, 357–381.

CIFELLI R. (1962) Some dynamic aspects of the distribution of planktonic foraminifera in the western North Atlantic. *Journal of Marine Research*, **20**, 201–213.

CURRY W. B., R. C. THUNELL and S. HONJO (1983) Seasonal changes in the isotopic composition planktonic foraminifera collected in Panama Basin sediment traps. *Earth and Planetary Science Letters*, **64**(1), 33–44.

DAVIES C. N. (1945) Definitive equations for the fluid resistance of spheres. *Proceedings of the Physics Society*, **57**, 259–270.

DEUSER W. G. (1986) Seasonal and interannual variations in deep-water particle fluxes in the Sargasso Sea and their relation to surface hydrography. *Deep-Sea Research*, **33**(2), 225–246.

DEUSER W. G. and E. H. ROSS (1981) Seasonal change in the flux of organic carbon to the deep Sargasso Sea. *Nature*, **283**, 364–365.

DEUSER W. G., E. H. ROSS, CH. HEMLEBEN and M. SPINDLER (1981) Seasonal changes in species composition, numbers, mass, size, and isotopic composition of planktonic foraminifera settling into the deep Sargasso Sea. *Paleogeography, Paleoclimatology, Paleoecology*, **33**, 103–127.

DIETRICH G., K. KALLE, W. KRAUSS and G. SIEDLER (1975) *Allgemeine Meereskunde*, Borntraeger, Stuttgart, 593 pp.

EREZ J., A. ALMOGI-LABIN and S. AVRAHAM (1991) On the life history of planktonic foraminifera: Lunar reproduction cycle in *Globigerinoides sacculifer* (Brady). *Paleoceanography*, **6**(3), 295–306.

FOK-PUN L. and P. D. KOMAR (1983) Settling velocities of planktonic foraminifera: density variations and shape effects. *Journal of Foraminiferal Research*, **13**, 60–68.

GIBBS R. J., M. D. MATHEWS and D. A. LINK (1971) The relationship between sphere size and settling velocity. *Journal of Sedimentary Petrology*, **41**, 7–18.

HEMLEBEN CH., M. SPINDLER and O. R. ANDERSON (1989) *Modern planktonic foraminifera*, Springer Verlag, Berlin, 363 pp.

HONJO S. (1978) Sedimentation of materials in the Sargasso Sea at a 5,367 m deep station. *Journal of Marine Research*, **36**, 469–492.

KIPP N. G. (1976) New transfer function for estimating past seasurface conditions from sea level distribution of planktonic Foraminifera in the North Atlantic. *Geological Society of America. Mem.*, **145**, 3–41.

KOMAR P. D. and C. E. REIMERS (1978) Grain shape effects on settling rates. *Journal of Geology*, **86**, 193–209.

KONTROVITZ M., K. C. KILMARTIN and S. W. SNYDER (1979) Threshold velocities of tests of planktic foraminifera. *Journal of Foraminiferal Research*, **9**, 228–232.

KREBS C. J., editor (1978) The experimental analysis of distribution and abundance. In: *Ecology*, 2nd edn., Harper & Row, New York, 678 pp.

MATTHÄUS (1972) Die Viskosität des Meerwassers. *Beitrag zur Meereskunde*, **29**, 93–107.

METZL N., B. MOORE III, A. PAPAUD and A. POISSON (1989) Transport and carbon exchange in Red Sea inverse methodology. *Global Biochemical Cycles*, **3**(1), 1–26.

OTT R., M. SIGNES, J. BIJMA and CH. HEMLEBEN (1992) A computer method for estimating volumes and surface areas of complex structures consisting of overlapping spheres. *Mathematical and Computer Modelling*, **16**.12, 83–98.

PARKER F. L. (1960) Living planktonic Foraminifera from the equatorial and southeast Pacific: Tohoku University. *Scientific Report Series* 2 (*Geology*) *Spec.*, **4**, 71–82.

REYNOLDS L. A. and R. C. THUNELL (1985) Seasonal succession of planktonic foraminifera in the subpolar North Pacific. *Journal of Foraminiferal Research*, **15**, 282–301.

REYNOLDS SAUTTER L. and R. C. THUNELL (1991) Planktonic foraminiferal response to upwelling and seasonal hydrographic conditions: Sediment trap results from San Pedro Basin, Southern California Bight. *Journal of Foraminiferal Research*, **21**(4), 347–363.

ROUSE H., editor (1949) *Elementary mechanics of fluids*, John Wiley & Sons. New York, 376 pp.

SCHULZ E. F., R. H. WILDE and M. L. ALBERTSON (1954) *Influence of shape on the fall velocity of sedimentary particles*. MRD Sediment Series, No. 5, CER 54ERS6, Colorado State University, 161 pp.

SIGNES J. M., J. BIJMA, CH. HEMLEBEN and R. OTT (1993) A model for the planktic foraminiferal shell growth. *Paleobiology*, **19**(1), 71–91.

TAKAHASHI K. (1984) *Measured and computed data for dimensions and sinking speeds of planktonic foraminifera from plankton tows and sediments*. SIO Reference Series, 84-17, pp. 1–42.

TAKAHASHI K. and A. W. H. BÉ (1984) Planktonic foraminifera: factors controlling sinking speeds. *Deep-Sea Research*, **31**, 1477–1500.

THUNELL R. C., W. B. CURRY and S. HONJO (1983) Seasonal variation in the flux of planktonic foraminifera: time series sediment trap results from the Panama Basin. *Earth and Planetary Science Letters*, **64**(1), 44–55.

THUNELL R. C. and S. HONJO (1981) Planktonic foraminiferal flux to the deep ocean: sediment trap results from the tropical Atlantic and the central Pacific. *Marine Geology*, **40**, 237–253.

VERCH N., M. UNGEWIS, K. SCHULZE and D. QUADFASEL (1989) MINDIK-RV METEOR cruise 5. CTD observations in the Red Sea and Gulf of Aden. (Unpublished Manuscript.)

VINCENT E. and W. H. BERGER (1981) Planktonic foraminifera and their use in paleoceanography. In: *The oceanic lithosphere: the sea*, Vol. 7, C. EMILIANI, editor, John Wiley & Sons, New York, pp. 1025–1119.